KfK 2944
April 1980

Pin Cooling and Dryout in Steady Local Boiling

A. J. Clare
Institut für Reaktorentwicklung
Projekt Schneller Brüter

Kernforschungszentrum Karlsruhe

KERNFORSCHUNGSZENTRUM KARLSRUHE
Institut für Reaktorentwicklung
Projekt Schneller Brüter

KfK 2944

Pin Cooling and Dryout in Steady Local Boiling

A.J. Clare[x]

[x] Delegated by Central Electricity Generating Board,
Berkeley, United Kingdom

Kernforschungszentrum Karlsruhe GmbH., Karlsruhe

Kernforschungszentrum Karlsruhe GmbH
ISSN 0303-4003

Pin Cooling and Dryout in Steady Local Boiling

Abstract

A study is presented of pin cooling and dryout mechanisms in steady local boiling, with the particular objective of understanding the substantial dryout margins observed in the KNS local boiling experiments. Mechanisms for the entry of liquid into the voided region are discussed, and pin cooling by draining liquid films deduced to be likely. The conditions required for interruption of the film flow, and hence for dryout, are examined, with particular attention to vapour/liquid interactions causing film breakdown, inhibition of rewetting and film flooding. This leads to the hypothesis that dryout occurs when a critical vapour velocity is reached, which is shown to be consistent with the limited data on dryout conditions in steady boiling.

Stabkühlung und Dryout bei stabilem lokalen Sieden

Zusammenfassung

Im Bericht werden die Mechanismen von Stabkühlung und Dryout bei stabilem lokalen Sieden untersucht, mit dem Ziel, die in den KNS-Versuchen beobachteten Dryout-Bedingungen zu verstehen. Mechanismen für den Eintritt von Flüssigkeit in den Dampfbereich werden diskutiert, wonach als wahrscheinlich angenommen wird, daß die Stäbe durch filmförmig herabfließende Flüssigkeit gekühlt werden. Es werden die Bedingungen untersucht, die zu einer Unterbrechung des Filmstromes und in der Folge zum Dryout führen. Besondere Beachtung wird dabei den Dampf/Flüssigkeits-Wechselwirkungen geschenkt, die eine solche Unterbrechung des Flüssigkeitsfilms verursachen und ein Wiederbenetzen und Nachfließen des Films verhindern. Diese Betrachtung führt zu der Hypothese, daß Dryout eintritt, wenn eine kritische Dampfgeschwindigkeit erreicht wird. Es wird gezeigt, daß diese Hypothese mit den verfügbaren experimentellen Daten über Dryoutbedingungen mit stabilem Sieden übereinstimmt.

Contents

1. Introduction

In the KNS local blockage experiments at KfK local boiling in sodium has been produced over a wide range of power and flow conditions with both a central (49 %) and a corner (21 %) blockage in a 169 pin bundle. Preliminary results from these experiments have been reported earlier /1,2/.

With both blockages the boiling was allowed to progress to permanent dryout conditions on a number of occasions, and substantial margins to dryout were observed.

In each case, at coolant flow rates of interest for normal reactor operation ($\geq$ 2 m/s), the boiling was initially steady, but at higher power/flow ratios it became oscillatory. In the central blockage case the initial steady boiling regime was restricted to a narrow band of conditions close to the start of boiling, and dryout occurred in the oscillating boiling regime. In the corner blockage case the steady boiling regime was very extensive, and a number of observations of dryout were made in this regime.

It was apparent that the onset of oscillations had the effect of appreciably increasing the dryout margin. Thus it is of some interest to be able to predict for particular cases whether the onset of dryout will be reached before the onset of oscillations.

The conditions for the onset of oscillatory behaviour will be discussed in a separate paper. Here the conditions for the onset of dryout in steady boiling are considered. The observations of dryout in steady boiling in the KNS corner blockage experiments are first summarized to provide a quantitative basis. An attempt is made to identify possible processes introducing liquid into the vapour region, in order to account for the dryout margins observed. Mechanisms for interrupting or inhibiting the liquid supply are examined with particular attention to interactions between vapour streams and draining liquid films which may cause dry patch formation or affect dry patch rewetting. Those most likely to be responsible for dryout in the steady boiling regime in the KNS experiments are identified.

2. Experimental observations of dryout

2.1 Steady boiling

An example of the development of the boiling region in a corner blockage experiment is given in figure 1. The coolant flow velocity is kept constant at 3 m/s in this experiment, and the pin power increased in steps, not all of which are shown in the figure. Boiling starts at a pin heat flux of 84 Wcm^{-2} and the size of the region within which thermocouples indicate the saturation temperature (the boiling region) increases with successive steps in pin power until permanent dryout is reached at a pin power of 128 Wcm^{-2}. Thus in this case a pin power increase of $\sim$50 % beyond start-of-boiling conditions is required to reach dryout.

Typical pin-wall thermocouple signals recorded in this experiment just after the final power step are shown in figure 2. Thermocouple K13 indicates the saturation temperature, showing small fluctuations of $\pm$ 1 ^{o}C with no definite periodicity and no discernible correlation with small fluctuations ($\sim \pm$ 2 mm) in the position of the void boundary. Thermocouple K11 shows examples of brief dryout events lasting $\sim$ 100 ms with temperature rises of $\sim$ 10^{o}C, before rewetting occurs. Such brief dryout indications are observed much earlier in the boiling development than permanent dryout. Thermocouple K24 shows a dryout event without subsequent rewetting, where the temperature continued to rise for $\sim$80^{o}C before the pin protection system tripped the power. In some experiments the power was tripped by a second protection system which monitors changes in the pin heater current. In these cases, too, permanent dryout is assumed to have occurred, but at a position where there is no thermocouple. In each case permanent dryout was a local event; at other positions in the void pin cooling was still adequate at the time the power was tripped.

Figure 3 and 4 show the boiling zones at permanent dryout conditions in experiments at various coolant flows and inlet temperatures. The experimental conditions for these cases are listed in Table 1, which also gives the results of void measurements at dryout conditions. The data will be considered in detail later; here we note only that dryout has been observed in boiling zones of various sizes and shapes and that the critical size of the boiling zone is clearly smaller for higher pin powers.

2.2 Oscillating Boiling

In boiling with a well developed oscillatory behaviour the motions of the void boundaries are large and the vapour volume varies almost sinusoidally with an amplitude of typically a few tens of cm^3. Figure 5 shows thermocouple signals recorded at dryout in such a case. The upper signal shows the periodic variations of the saturation temperature (freq. $\sim$ 5 Hz, amplitude $\sim 7^oC$) with, in this position, no signs of dryout. Another thermocouple shows that dryout occurs exactly in phase with the oscillations in size, beginning during the void expansion and terminating during the void contraction, without, however, being immersed in subcooled liquid. Eventually the rewetting during void contraction fails and the power is tripped due to large temperature increases. In this case the rewetting process before permanent dryout occurs is complicated by the large motion of the void interface and for this reason is not discussed further below.

3. Models of the steady boiling zone

3.1 Requirements of a model

We consider here possible models for the simpler case of the steady boiling zone where motions of the void interface may be neglected. It is clear, both from the large dryout margins observed and from signals obtained from Chen-type void meters, that the boiling zone contains much liquid; this could be in the form either of droplets or of liquid films. That the liquid is at or very close to the saturation temperature is indicated by the thermocouple signals.

The basic requirements of a pin cooling/dryout model are

a) to explain how the liquid enters the voided zone, and
b) to explain how the pins are cooled and how the cooling is eventually prevented.

Possible approaches are discussed in the following sections.

3.2 Liquid supply mechanisms

3.2.1 Draining film hypothesis

One hypothesis to explain how liquid enters the voided region is that it enters in the form of liquid films on the pins, as illustrated in figure 6. At the point of impingement of the liquid stream on a pin surface at the void boundary conservation of momentum implies a significant momentum flux of liquid along the pin into the void. Liquid entering at the top will be further accelerated by gravity, in the absence of other interactions, whilst liquid entering from below will be rapidly decelerated and penetration is therefore very small (1 cm). Supply of liquid in this way to a gas void has been observed, and its magnitude investigated, by Clare and Board /3/. Their experiments in water with pins of a similar size to those of interest here suggest that a liquid supply rate of about 1-3 $cm^3 s^{-1}$ per pin may be expected at coolant flow rates at the void boundary in the range 2-4 m/s. In comparison with this, the pin powers and exposed pin lengths at dryout in the cases given in table 1 and figures 3 and 4 imply a liquid supply rate $\geq$ 0.5 $cm^3 s^{-1}$ per pin. Thus if we supposed that the measurements reported in /3/ may be applied in local boiling in sodium, this liquid supply mechanism alone would probably be sufficient to account for the pin cooling in the observed steady vapour regions.

3.2.2 Two-phase mixture model

The basic features of this hypothesis are illustrated in figure 7. It is assumed that the fluid in the reverse flow heats up to the saturation temperature and that a small component of the flow crosses the saturation isotherm. As the saturation isotherm is traversed small vapour bubbles form and expand rapidly on further heating, breaking up the flow into a mixture of droplets and vapour which must expand and accelerate towards the main condensation surfaces. It is observed experimentally that the upper and outer interfaces of the void are locations of steep temperature gradient and high turbulence (because of the shear layer produced by the edge of the blockage), and that they also represent a large proportion of the void surface area. Thus the predominant direction of flow in the void is likely to be towards these surfaces.

This hypothesis may be treated using a simple homogeneous boiling model applied to the recirculating wake. A subchannel code employing such a model would be needed to calculate the coolant mass flow into the boiling zone; we do not attempt to estimate it here. However, some approximate evaluations of the minimum mass flows required to account for pin cooling in the observed boiling regions, and also of the associated two-phase pressure drops, have been attempted. For this purpose we consider the boiling region at an axial position where the two-phase flow within it is predominantly radial, beginning at the inner boundary at radius r_{ib} *where the mass flux across the saturation isotherm is* $\dot{m}_{ib}$. *The energy conservation equation yields the mass fraction of vapour, x, as a function of radial position, r:*

$$x = \frac{\alpha_1 \, q}{2\dot{m}_{ib} \, r_{ib} \, h_{fg}} \, (r^2 - r_{ib}^2),$$

where h_{fg} *is the latent heat of vapourisation, q the pin heat flux and* α_1 *the pin surface area per unit total volume. For* $x \leq 1$ *at the outer boundary,* r_{ob}, *of the boiling region*

$$\dot{m}_{ib} \geq \frac{\alpha_1 \, q}{2r_{ib} \, h_{fg}} \, (r_{ob}^2 - r_{ib}^2),$$

which for typical cases at dryout requires

$$\dot{m}_{ib} \geq 0.5 \text{ gm s}^{-1} \text{ cm}^{-2}.$$

Following Owens /4/ we estimate the 2-phase pressure drop across the boiling region with the assumptions of homogeneous 2-phase flow and using the single phase friction factor. The latter is obtained from the correlation of Gunter and Shaw /5/ for cross flow over bare tube banks. These assumptions lead, neglecting pressure-dependent terms, to a pressure gradient at radius r of

$$\frac{dP}{dr} = F_{T.P.} \, \frac{\dot{m}_{ib}^2 r_{ib}^2}{r^2} \, V_f(1+\Gamma x) + \frac{\dot{m}_{ib}^2 r_{ib}^2}{\alpha_2 r^2} \, V_f \left[\Gamma \frac{dx}{dr} - (1+\Gamma x) \right]$$

where α_2 *is the mean ratio of flow area to total area in the bundle,* v_g *and* v_f *are the specific volumes of the vapour and liquid phases,* $\Gamma = \frac{v_g}{v_f} - 1$, *and* $F_{T.P}$ *is obtained from /5/. Substituting for x from above and integrating across the boiling region gives for the pressure drop*

$$\Delta P = \frac{\dot{m}_{ib} r_{ib} V_f \Gamma \alpha_1 q}{2 h_{fg}} \left\{ \frac{2}{\alpha_2} \ell n \left(\frac{r_{ob}}{r_{ib}} \right) + \left(F_{T.P.} - \frac{1}{\alpha_2} \right) \frac{(r_{ob} - r_{ib})^2}{r_o} \right\}$$

Evaluating for typical cases and using $\dot{m}_i \geq 0.5$ *gm* s^{-1} cm^{-2}, *from above, we obtain the result*

$$\Delta P \geq 1.5 \times 10^{-3} \text{ bar}$$

$$= 0.1^{o}C \quad \text{in saturation temperature.}$$

The thermocouples in the boiling region show a scatter of $\pm 2^{o}C$ *in measured saturation temperatures with no consistent trend. Thus if the observed boiling regions were of the form of a radially flowing 2-phase mixture, sufficient to provide cooling up to dryout conditions, this would not require improbably high mass fluxes or imply radial pressure drops which could be detected in the KNS experiments.*

The liquid distribution in 2-phase cross flow is likely to be strongly influenced by the process of droplet deposition on the pin surface, and, at higher vapour velocities, the competing process of droplet entrainment in the vapour flow. Processes of this sort have been studied with water droplet sprays in an air stream directed at single pins in cross flow /6,7/. It is clear from these studies that, at vapour velocities below the entrainment threshold, pins are very efficient collectors of liquid droplets, the deposited liquid then forming into a draining liquid film. In view of this it seems unlikely that a homogeneous 2-phase model would be capable of correctly predicting the liquid distribution in the boiling region.

Apart from uncertainties about the liquid distribution, the 2-phase mixture model implies a marked increase of void number towards the condensation surfaces, and first indications of dryout would be expected close to these surfaces since the pins here would be the first to suffer deprivation of the liquid supply.

With reference to the experimental results in figures 3 and 4 it is clear that in five out of the six cases dryout (observed or inferred) occurs in the vicinity of the outer boundary which we expect to be the main condensation interface. In one case (Expt. 215/1) dryout occurs in the centre of

the boiling zone. As regards the void number, two cases can be distinguished from the data in Table 1. In the boiling regions at 2 m/s flow rate, which extend into the corner of the test section, no clear radial or axial trend is found. In the other cases, where a reverse flow in the corner persists, an increase in void number towards the outer boundary is apparent at each axial level. Thus there is some qualitative support for the 2-phase mixture hypothesis, but there are also significant exceptions.

In summary it may be said that at present it is not possible to be sure which is the main mechanism supplying the voided zone with liquid. Quantification of the 2-phase mass flows in the boiling region using a subchannel code like SABRE would be of particular interest in this connection. Observations of pin dryout in a gas void in subcooled sodium could possibly indicate the contribution of liquid draining from the upper void boundary since in this case the other source does not operate.

3.3 Dryout Mechanisms

In the previous section it was seen that liquid which enters the void, by whatever mechanism, is likely to form draining films on the pins which are able to dissipate heat by evaporating the liquid. Whilst it is not yet clear which of the liquid supply mechanisms is dominant, the film entry mechanism has been roughly quantified in water experiments and appears to be sufficient to make pin dryout by total evaporation of the supply improbable. In this section we examine dryout mechanisms which depend on interruption or instability of the film flow.

3.3.1 Film flow instability

If the film breaks up into separate rivulets some of the pin surface will remain uncooled. The condition for spontaneous breakup into rivulets has been examined by Bankoff /8/ on the basis of an equal total energy (kinetic + surface) criterion. His analysis, for laminar flow, indicates that the minimum film thickness for a stable film depends on the wetting properties of the surface, but for sodium in well wetted conditions it is 2×10^{-4} cm. This is so thin that the onset of film instability would be indistinguishable from the onset of total evaporation at typical pin powers in local boiling.

3.3.2 Dry patch instability

Occurrences of brief dryout appear much earlier in the boiling development than permanent dryout. At first these dry patches, however produced, are rewetted after a time of about 100 ms . Since permanent dryout has been observed only as a local event within the void it is possible that it occurs where local conditions prevent the rewetting of a dry patch.

The stability of dry patches in isothermal conditions has been examined by Hartley & Murgatroyd /9/ and Murgatroyd /10/ who consider both the force balance and the minimum energy condition at the upstream stagnation point of a dry patch in a gravity draining laminar film, and also in films driven by shear forces at the gas/liquid interface. Rewetting is possible if the stagnation pressure is able to overcome the surface tension forces which oppose the advance of the film over the dry patch. Zuber & Staub /11/ show that if the surface is heated, thermal effects arising from the temperature dependence of the surface tension and from evaporation thrust may be important. In the present case, however, the pin heat flux is not high enough for these effects to be very significant. Rewetting may however be further inhibited if there is an adequate vapour counterflow which both reduces the film velocity and exerts a restraining pressure on the exposed edge of the liquid film.

For the present purposes the Hartley and Murgatroyd analysis is modified (see Appendix) to allow for the effects on the film velocity profile of both gravity and vapour counterflow which are of the same order of magnitude. Except in conditions approaching flooding, it is found that the critical liquid flow for dry patch rewetting is rather insensitive to the counterflow, but very sensitive to contact angle (see Figure 9). For the film flow rates of interest here ($Q \simeq 2$ cm^{3}s^{-1}, but certainly > 0.5 cm^{3}s^{-1}) dry patch rewetting could be prevented either by a large contact angle ($\theta > 60^{\circ}$) or by a vapour counterflow approaching the flooding limit.

We note that if dry patch rewetting is delayed the surface temperature in the dry area may rise to a level where the rewetting front is controlled by other factors, such as boiling, and the rewetting rate could be limited by heat conduction effects rather than hydrodynamics. The relevant surface

temperature is not well known but is likely to be > T_{sat} + 70°C; this would be at or above the trip level for the KNS pins and is thus unlikely to be reached in these experiments.

Measurements of the contact angle for sodium at ∿ 920°C are not available. Bader & Busse /13/ have measured the static wetting angle of sodium in a vapour atmosphere on various surfaces, including stainless steel, at temperatures upto 720°C, and report very low angles, < 5°, for temperatures above ∿ 500°C. The contact angle at a moving rewetting front may be very different from the static contact angle, but the observed successful rewetting over a wide range of conditions before permanent dryout implies that a high contact angle is not the primary reason for dryout.

Film flooding due to gas or vapour counterflow has received considerable attention. It is known from experimental observations /14,15,16/ of countercurrent film flow that the liquid interface remains smooth and the film thickness approximately constant for countercurrent gas phase flows upto near the flooding condition. At some point, as the gas phase velocity is increased, waves appear on the film surface which grow and are entrained in the gas flow, or may, in small channels, form liquid bridges which are accelerated upwards and disintegrate into droplets. The surface waves increase the surface shear force so that the film mean velocity may be reduced to zero, which is the flooding condition. Grolmes et al. /15/ report measurements of the interfacial shear stress coefficient at the flooding point with various liquids, leading to the correlation

$$f_i = 0.006 + 200\ \delta^2 \left(\frac{\mu}{\mu_R}\right)^{-0.44}, \qquad (\mu_R = 1\ c.p.)$$

where δ (cm) is the undisturbed film thickness. Use of this correlation to evaluate the interfacial shear stress

$$\tau_i = f_i \ \frac{1}{2}\ \rho_v u_v^2$$

in equation (A3) for the mean velocity of a laminar film draining under gravity, gives the critical vapour velocity for flooding:

$$u_v = \frac{2}{\sqrt{3}} \sqrt{\frac{\rho_L}{\rho_v}} \sqrt{\frac{g\,\delta}{f_i}} \quad .$$

For sodium film flow rates of 1-3 $cm^3 s^{-1}$ per pin, u_v = 580-490 cm s^{-1}.

Thus if the upward axial component of the vapour velocity reaches $\sim$ 500 cm s^{-1} permanent dryout could result from film flooding. However, in a locality where dry patches are formed, permanent dryout could arise from prevention of re-wetting at a slightly lower axial vapour velocity.

3.3.3 Effects of vapour cross flow

The cross flow component of the vapour stream is likely to be large in local boiling because the main area for condensation is the outer edge of the wake. Possibly important processes to be considered are dry patch formation, and liquid redistribution by entrainment and redeposition. Referring to the following sketch, film thinning and dry patch formation could be expected at D; whilst liquid droplet entrainment might be possible at A,B and C with some redeposition at D. Here we attempt

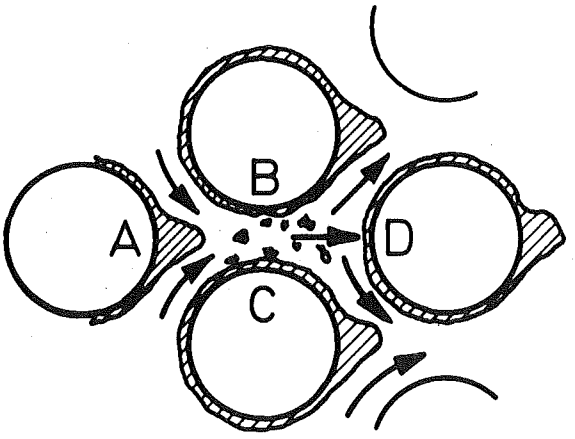

to estimate the vapour velocities at which these processes may become important.

The conditions required to produce film breakdown by a vapour stream impinging in a direction normal to a liquid film are given approximately by the relative magnitudes of the vapour and liquid stagnation pressures. Breakdown might be expected if

$$\frac{1}{2} \rho_v u_v^2 \geq \frac{1}{2} \rho_L \bar{u}_L^2 \quad ,$$

or, assuming the film flow is laminar,

$$u_v \geq \sqrt{\frac{\rho_L}{\rho_v}} \left(\frac{Q}{\pi d}\right)^{2/3} \left(\frac{\rho_L g}{3\mu}\right)^{1/3} \qquad (1)$$

To confirm this a simple isothermal experiment was performed using water draining down a smooth, vertical, 6 mm diameter stainless steel rod, with a horizontal jet (4 mm diameter) of argon gas directed at it. With a constant water flow rate, increasing the gas velocity from zero produced, at first, a local thinning of the film until a clearly defined thin patch was formed with a pronounced step at the upper liquid stagnation point. The diverted liquid flowed in a band of thickened film on each side of the thin patch. At some higher gas velocity the thin patch broke down. Figure 10 shows the measured critical gas velocities for visible thin patch formation and for film breakdown, as functions of the liquid volumetric flow rate Q. The curve representing equation (1) is included for comparison, and appears to form an upper bound to the critical velocity for film breakdown.

The formation of a thin patch at considerably lower (< 0.3) gas velocities suggests that in the case of a heated pin, the creation of a dry patch due to evaporation could occur at vapour velocities appreciably lower than those predicted by equation (1).

For a sodium film flow of $Q = 1\ cm^3 s^{-1}$ on a 6 mm diameter pin, equation (1) predicts film breakdown at an impinging vapour velocity of about 1450 $cm\ s^{-1}$. This might be reduced to perhaps $\sim 500\ cm\ s^{-1}$ by evaporation at a thin patch, though this remains uncertain in the absence of experimental confirmation.

Observations of liquid entrainment in the above water experiment are of some interest. Liquid droplets were seen to be detached from the thickened film around the sides of the thin patch, in some cases. For liquid flow rates $Q < 6\ cm^3 s^{-1}$ no entrainment was observed before film breakdown. At higher liquid flow rates entrainment began before film breakdown, at a gas velocity of $\sim 1700\ cm\ s^{-1}$.

This observation falls within the scatter shown by the results of cross flow entrainment experiments reported by Barnard et al. /6/ for a greater, but overlapping, range of film Reynolds number, but with pins of larger diameter. This limited amount of data on cross flow entrainment from draining liquid films suggests that at the sodium film Reynolds numbers of interest here ($Re_f \tilde{=} 10^3$) entrainment would begin at cross flow vapour velocities >1500cm s^{-1}.

3.3.4 Summary of dryout mechanisms

From the above discussion it is clear that in both axial and cross flow vapour streams, interactions leading to dryout became important at lower vapour velocities than those required for significant entrainment, so that the treatment of the liquid and the vapour as essentially separate phases is justified.

Secondly, it is evident that dry patches could be formed by the cross flow vapour stream. The early appearance of brief dryout could be explained if the film flow rate and the vapour velocity are both fluctuating quantities which occasionally, but briefly, produce conditions favourable for local film breakdown, although the mean vapour velocities are insufficient to prevent rewetting. Rewetting remains possible unless the axial vapour velocity persists at approximately 500 cm s^{-1}, or the cross flow velocity persists at a more uncertain critical level, but probably in the range 500-1450 cm s^{-1}. Failure to rewet would lead to local permanent dryout. In the absence of dry patch formation dryout would result from liquid film flooding at a similar critical velocity of the axial vapour flow.

This hypothesis leads to the prediction that permanent dryout should occur when the maximum velocity in the void reaches the critical value, which may be sensitive to the direction of vapour flow. The maximum vapour velocities will be reached near the void boundary in the regions of highest condensation rate adjacent to the turbulent shear layer at the edge of the wake. They cannot be evaluated for real cases. Instead the mean vapour velocity at the void boundary is estimated using

$$\rho_v \, h_{fg} \, \bar{u}_v = \frac{\alpha_1}{\alpha_2} \, q \, \frac{V}{S} ,$$

or, at dryout conditions

$$\left(\frac{V}{S}\right)_{DO} = \frac{1}{q_{DO}} \bar{u}_v(crit) \frac{\alpha_2}{\alpha_1} \rho_v h_{fg} \qquad (2)$$

In figure 11 the approximate values of $\left(\frac{V}{S}\right)_{DO}$ obtained from figures 3 and 4 are plotted against $1/q_{DO}$. In most of these cases dryout occurred shortly (< 10 s) after a power increase, before equilibrium was reached, and the dryout conditions are assumed to lie between those of the final two steps. This provides the uncertainty indicated in the figure. In two cases dryout occurred at the equilibrium conditions of the step, > 20 s after the power increase. Uncertainties in the void size and shape are not included.

This rather limited quantity of data shows quite good agreement with the form of equation (2), in that the points lie closely scattered about a straight line through the origin. The best line through the origin and the points, shown in figure 11, corresponds to a mean vapour velocity at the boundary of

$$\bar{u}_v\ (crit) = 420\ cm\ s^{-1}\ ,$$

consistent with an expected maximum vapour velocity of $\gtrsim 500\ cm\ s^{-1}$. A third point of agreement is the location of observed dryout events in most cases close to the void outer boundary, where the maximum velocities are expected.

Thus the experimental dryout conditions in steady boiling support the hypothesis that dryout is induced when the vapour velocity is high enough to prevent dry patch rewetting, or possibly to cause film flooding.

Figure 11 provides a semi-empirical relation between the void volume/surface area ratio and the pin heat flux at dryout conditions. In view of the small amount of data and the uncertainties in critical vapour velocities, particularly in cross flow, this relation can be considered valid only for voids of similar shape to those represented in the data, and for similar directions of vapour flow. Within these restrictions figure 11 may form the basis for an approximate extrapolation to different blockage sizes and pin powers, provided a means of calculating the void region exists.

An implication of the above analysis is that the prediction of dryout in a local boiling code may require a boiling model capable of representing interactions between liquid films and the vapour stream, and is likely to depend on an accurate prediction of the direction of vapour flow. This in turn requires an adequate calculation of the temperature and turbulence fields in the liquid around the boiling region, since these determine the main areas for condensation.

4. Conclusions

1. *Experimental results relating to permanent dryout in steady local boiling in the KNS blockage experiments have been presented. An attempt has been made to identify the dominant mechanisms involved in:*

   - *supplying the pins in the boiling region with adequate liquid to account for large dryout margins,*

   - *the onset of dryout.*

2. *A liquid supply model based on an expanding, accelerating 2-phase mixture derived from the reverse flow is difficult to assess without further theoretical and experimental effort. Liquid supplied in the form of a draining film from the upper boundary has been approximately quantified in water experiments, and the supply rates are probably sufficient to provide pin cooling requirements beyond the observed dryout conditions in steady boiling.*

3. *Interactions between a draining liquid film and a countercurrent or cross flow vapour stream have been examined. For each case the vapour velocities needed for film breakdown or prevention of dry patch rewetting have been approximately evaluated.*

4. *It has been shown that the dryout conditions observed in steady boiling in the KNS experiments are consistent with the hypothesis that dryout is induced when the critical vapour velocity for preventing dry patch rewetting, or for film flooding, is reached.*

5. *The hypothesis provides a basis for applying the KNS data to different blockage sizes and pin powers if the vapour region can be calculated, and if the void shape and direction of vapour flow are not very different from those represented by the data.*

Nomenclature

d *pin diameter*

D_h *subchannel hydraulic diameter*

f_i *interface friction coefficient*

$F_{T.P}$ *two-phase friction coefficient*

g *gravitational acceleration*

h_{fg} *latent heat of vapourisation*

K_V *void number*

L *flow diversion length above dry patch*

$\dot{m}, \dot{m}_{ib}$ *mass flux and its value at void inner boundary*

P *pressure*

q, q_{SB} *pin heat flux and its value at start of boiling*

Q *liquid film volumetric flow rate*

R *dry patch radius*

Re_f *film Reynolds number*

r, r_{ib}, r_{ob} *radial position and its values at the void inner and outer boundaries*

S *void surface area (excluding pins)*

T_{in}, T_{sat} *inlet temperature, saturation temperature*

t	*time*
$u_y, \bar{u}_L$	*liquid velocity at position y in film, average velocity in film*
$u_v, \bar{u}_v$	*vapour velocity, average value at void boundary*
U_o	*mean sodium velocity at test section inlet*
v_f, v_g	*specific volumes of liquid and vapour phases*
V	*vapour volume (excluding pins)*
x	*vapour mass fraction*
y	*coordinate perpendicular to pin surface*
z	*axial coordinate*
α_1	*pin surface area per unit total volume*
α_2	*ratio free area/total area in cluster*
Γ	$= \frac{v_g}{v_f} - 1$
δ	*film thickness*
θ	*contact angle*
μ	*liquid viscosity*
ρ_L, ρ_V	*liquid density, vapour density*
σ	*surface tension of liquid*
τ_i, τ_w	*shear stress in film at interface and at wall.*

References

/1/ *Huber F., Peppler W.: Form and development of boiling behind a 49% central blockage, 7th LMBWG Meeting, Petten, June 1977.*

/2/ *Clare A.J. et al.: Preliminary results of the temperature distribution and boiling behaviour behind a wall blockage in a 169 pin bundle, 8th LMBWG Meeting, Mol, October 1978.*

/3/ *Clare A.J., Board S.J.: A study of gas/vapour cavities and the implications for local boiling propagation, 6th LMBWG Meeting, 1975*

/4/ *Owens W.L.: International Developments in Heat Transfer, PtII, ASME, 363-368, 1961.*

/5/ *Gunter A.Y., Shaw W.A.: Trans ASME, 67, 643-660, 1945*

/6/ *Barnard D.A., Ward J.A., Whalley P.B.: Paper presented at 6th Water Reactor Safety Research Information Meeting, Gaithersburg, Nov. 1978*

/7/ *Dallman J.C., Kirchner W.C., Starkovich V.: Paper presented at 6th Water Reactor Safety Research Information Meeting, Gaithersburg, Nov. 1978*

/8/ *Bankoff S.J.: International Journal Heat Mass Transfer, 14 , 2143-46, 1971*

/9/ *Hartley D.E., Murgatroyd W.: International Journal Heat Mass Transfer, 7, 1003-1015, 1964*

/10/ *Murgatroyd W.: International Journal Heat Mass Transfer, 8, 297-301, 1965*

/11/ *Zuber N., Staub F.W.: International Journal Heat Mass Transfer, 9, 897-905, 1966*

/12/ Gimbutis G.I., Vasilyauskas V.P., Shinkunas S.S.: Teploenergetika, 20(4), 75-77, 1973 (Translation UDC 532.5: 536.24).

/13/ Bader M., Busse C.A.: J. Nuclear Materials, 67, 295-300, 1977.

/14/ Hewitt G.F., Wallis G.B.: UKAEA Report AERE-R4022, 1963.

/15/ Grolmes M.A., Lambert, Fauske H.K.: Inst. Chem. Eng. Symp. Series No. 38, Proc. Symp. 'Multiphase Flow Systems', Glasgow, 1974.

/16/ Duffey R.B., Ackermann M.C., Piggott B.D.G., Fairbairn S.A.: CEGB Report RD/N3667, 1976.

Appendix: Dry patch rewetting in vapour counterflow conditions

Following Hartley & Murgatroyd we consider the pressure change along an infinitesimally thin element (Figure 8) along the streamline from E, where the film velocity is undisturbed, to the stagnation point G at the upper boundary of the dry patch, a distance L;

$$P_G - P_E = \frac{1}{2}\rho_L \frac{1}{\delta}\int_o^\delta u_y^2\, dy + \rho_L g L - \frac{1}{\delta}\int_E^G (\tau_w + \tau_i)\, dz$$

where τ_w and τ_i are respectively the wall and interfacial shear stresses. The latter, τ_i, is constant over EG, but τ_w reduces to zero at the stagnation point G. In order to obtain an estimate of the imbalance of shear stresses over EG we suppose that τ_w reduces linearly to zero from its equilibrium value at E, thus

$$\tau_w = (\delta\rho_L g - \tau_i)\left(1 - \frac{z}{L}\right) \quad ,$$

measuring z from E. We further suppose that a typical dryout patch might have a radius (R) similar to the pin radius (i.e. the patch is restricted to one side of the pin) and that the flow diversion length L is also similar; thus

$$L = R = \frac{d}{2} \quad .$$

We then obtain

$$(P_G - P_E)_L = \frac{\rho_L}{2\delta}\int_o^\delta u_y^2\, dy + (\rho_L g\delta - \tau_i)\frac{d}{4\delta} \quad .$$

On the vapour side we have

$$(P_G - P_E)_V = \frac{4\,\tau_i L}{D_h} + C\,\frac{1}{2}\rho_v u_v^2$$

where D_h is the hydraulic diameter of the channel available for vapour flow, and C represents the effects of the step. We note that if the contact angle, $\theta = 90^o$, $C = 1$, and if $\theta = 0$, $C = 0$; it is proposed therefore to represent C roughly by the function

$$C = 1 - \cos\theta \quad ,$$

giving

$$(P_G - P_E)_V \cong \frac{2d}{D_h} \tau_i + (1 - \cos \theta) \frac{1}{2} \rho_V u_V^2 \quad .$$

At the critical rewetting conditions the excess pressure on the liquid side at G must be balanced by the surface tension at the film surface, and we obtain the result that rewetting is possible if

$$(P_G - P_E)_L - (P_G - P_E)_V \geq \frac{\sigma(1 - \cos \theta)}{\delta} \quad ;$$

i.e., if

$$\frac{\rho_L}{2\delta} \int_0^\delta u_y^2 \, dy \geq (1 - \cos \theta) \left(\frac{\sigma}{\delta} + \frac{1}{2} \rho_V u_V^2 \right)$$

$$- (\rho_L g \delta - \tau_i) \frac{d}{4\delta} + \frac{2d}{D_h} \tau_i \quad .$$

On comparison of terms we find that those representing the pressure drop on the vapour side may be neglected and the rewetting criterion becomes

$$\frac{\rho_L}{2} \int_0^\delta u_y^2 \, dy \geq \sigma(1 - \cos \theta) - (\rho_L g \delta - \tau_i) \frac{d}{4} \quad . \qquad (A1)$$

In choosing a suitable film velocity profile, u_y, we note that for volumetric flow rates $Q < 3$ cm^{3}s^{-1} (per pin) the film Reynolds number is $Re_f < 3 \times 10^3$, and experimental results /e.g. 12/ indicate that the Nusselt laminar flow theory is applicable for the equilibrium velocity profile. It is unlikely that fully developed film flow conditions are reached in the boiling zone, where distances are short and the vapour flow velocities are spatially variable, but a laminar profile will be used in these approximate calculations. The velocity profile for a gravity draining film with opposing interfacial shear is then

$$u_y = \frac{\rho_L g}{2\mu} (2y\delta - y^2) - \frac{\tau_i}{\mu} y, \qquad (A2)$$

and the mean film velocity is

$$\bar{u}_L = \frac{\rho_L g \delta^2}{3\mu} - \frac{\tau_i}{2\mu}\,\delta \quad . \qquad (A3)$$

Equation (A3) gives the condition for film flooding ($\bar{u}_L = 0$) as

$$\frac{2\tau_i}{\rho_L g} = \frac{4\delta}{3}$$

and we require, therefore, to solve the hydrodynamic rewetting criterion, equation (A1), obtaining the critical film thickness in the range of counter-flow conditions

$$\frac{2\tau_i}{\rho_L g} < \frac{4\delta}{3}$$

We observe from equation (A2) that there is a surface layer of the film

$$y > \delta - \frac{2\tau_i}{\rho_L g}$$

within which the velocity is negative. This complicates the evaluation of the stagnation pressure, and in order to obtain a positive stagnation pressure for all $\bar{u}_L > 0$ we use the approximation

$$\int_0^\delta u_y^2\, dy \cong \bar{u}_L^2\, \delta$$

$$= \left(\frac{\rho_L g}{2\mu}\right)^2 \left[\frac{4\delta^5}{9} - \frac{2}{3}\left(\frac{2\tau_i}{\rho_L g}\right)\delta^4 + \frac{1}{4}\left(\frac{2\tau_i}{\rho_L g}\right)^2 \delta^3\right]$$

Results are given in figure 9 for contact angles 10^o-60^o, and instead of the critical film thickness the critical liquid flow rate

$$Q_{crit} = \pi\, d\, (\bar{u}_L \delta)_{crit}$$

is plotted.

Table 1: *Dryout conditions in steady boiling*

Expt.	215/2	216/3	214/2	215/1	216/2	214/1
Run	466	491	403	458	485	393
U_o m/s	2.01	2.02	3.00	3.02	3.03	4.00
q Wcm^{-2}	97.0	79.1	135.0	128.1	106.8	165.0
q_{SB} Wcm^{-2}	63.7	49.3	95.1	84.2	64.8	120.5
T_{in} ^oC	503	586	425	496	580	421
Position z/subchan.	Void measurements* at dryout conditions					
10/3	.306	.333	-.007	-.007	-.012	-.012
7	.477	.387	-.107	-.106	-.079	-.042
30/3	.305	.343	-.009	-.017	.49	-.011
7	.074	.192	-.019	.024	.202	-.026
8	.300	.405	-.015	.156	.420	.001
9	.294	.255	.587	.677	.540	.168
50/3	.142	.230	.058	.063	.032	.013
7	.284	.415	-.010	.204	.319	-.012
70/7	.160	.181	.048	.035	.010	.018
7	.083	.081	.093	.066	.050	.140

* The values given here are

$$K_V \text{ (dryout)} - K_V \text{ (single-phase)}$$

where the void number K_V is given by

$$K_V = \frac{\text{mean Chen probe signal}}{\text{max. Chen-probe signal (when dry)}}$$

Experiment 215/1 $q_{SB} = 84\ Wcm^{-2}$ $U_0 = 3\ m/s$
$T_{in} = 500\ °C$

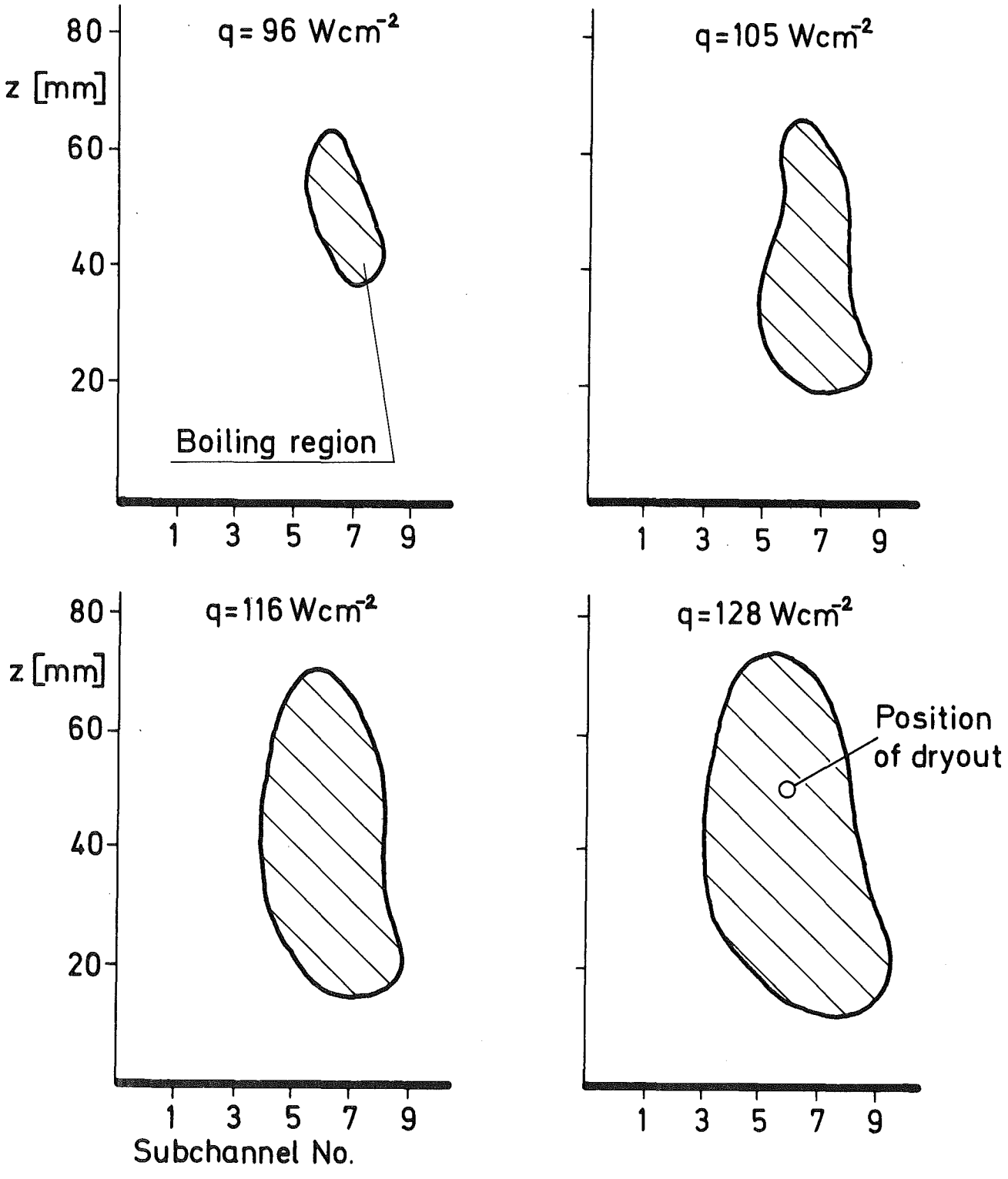

Fig.1 Development of a boiling region in steady boiling

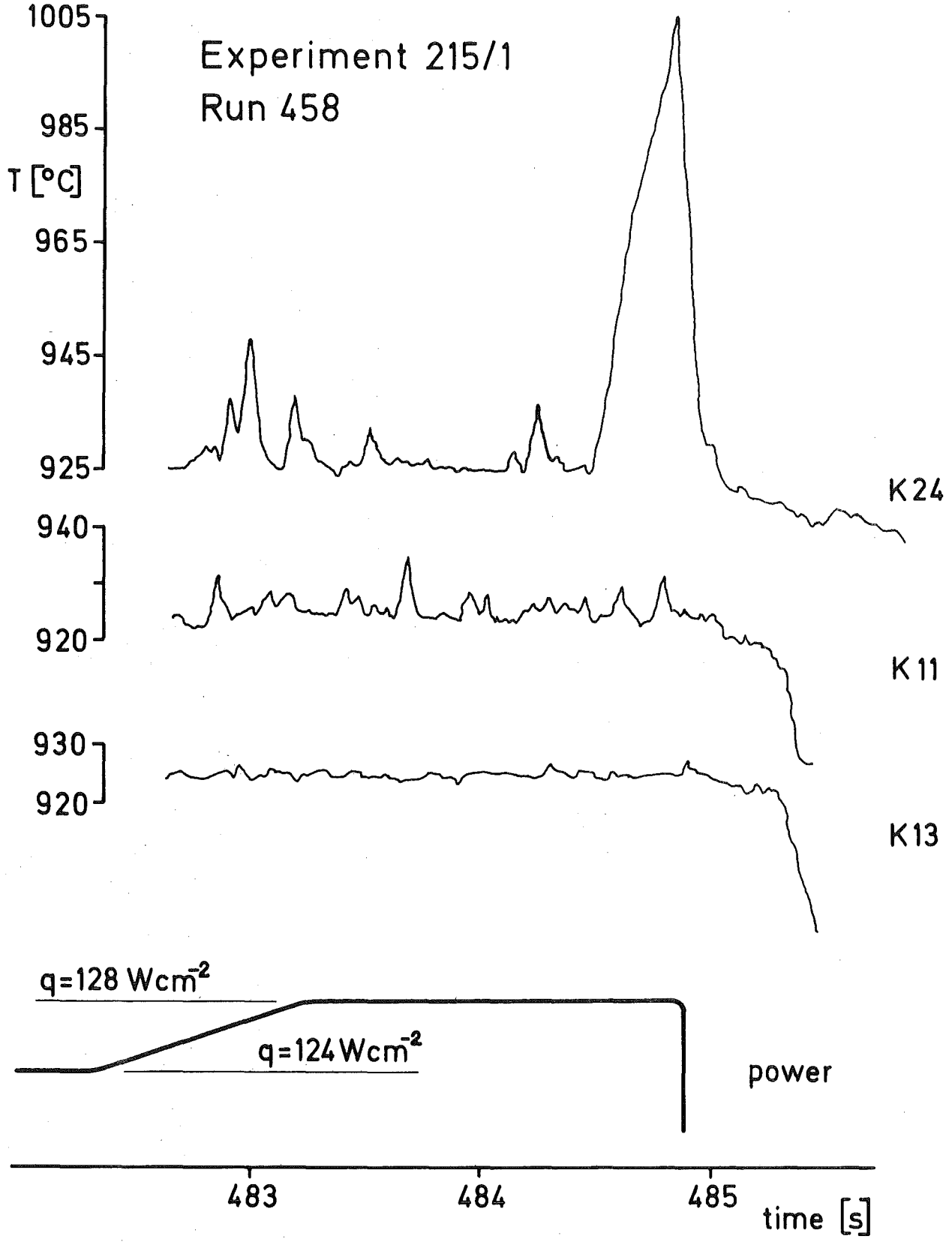

Fig.2 Thermocouple signals at dryout in steady boiling

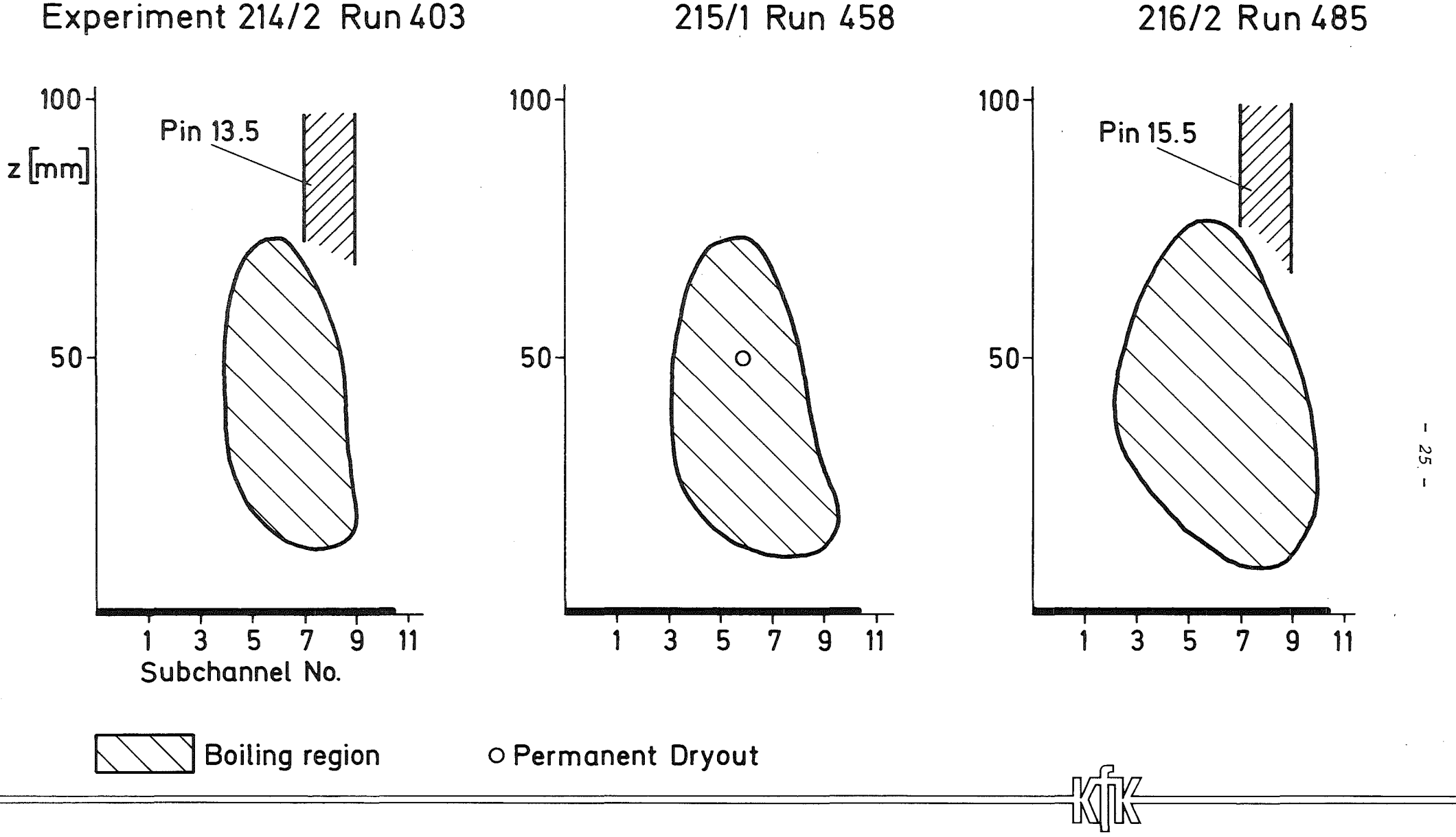

Fig.3 Boiling regions at dryout conditions

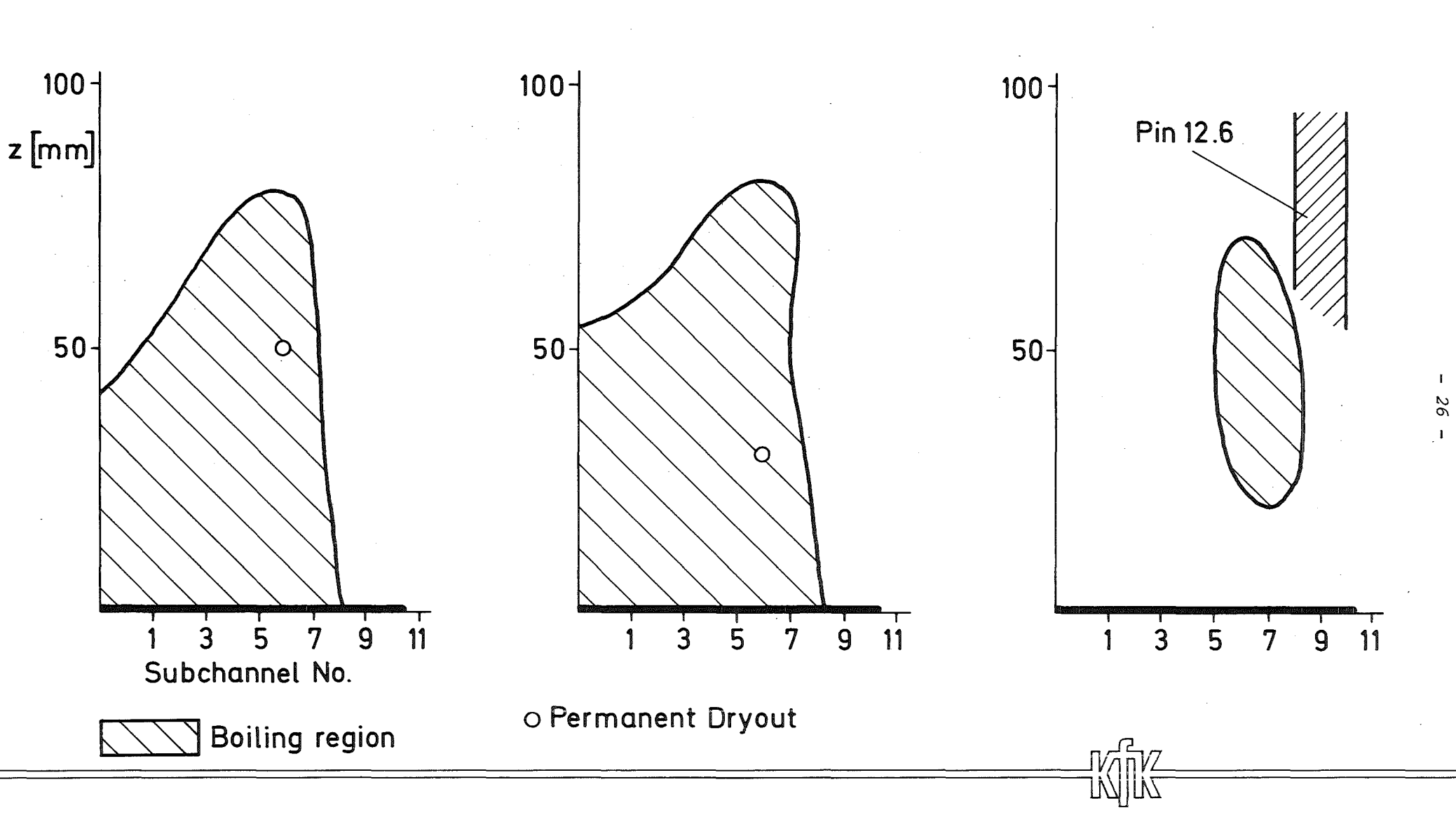

Fig.4 Boiling regions at dryout conditions

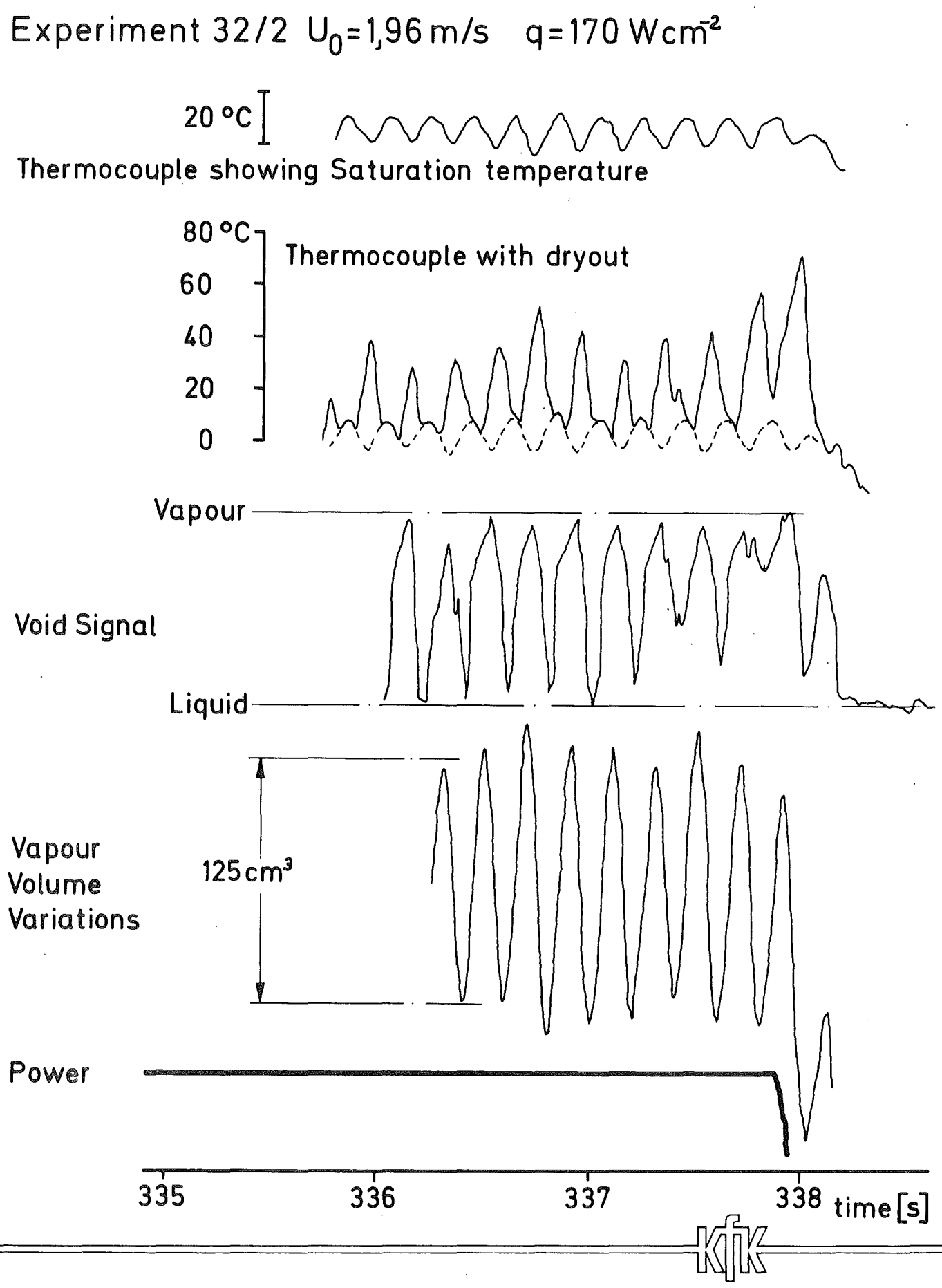

Fig.5 Signals at dryout in oscillating boiling

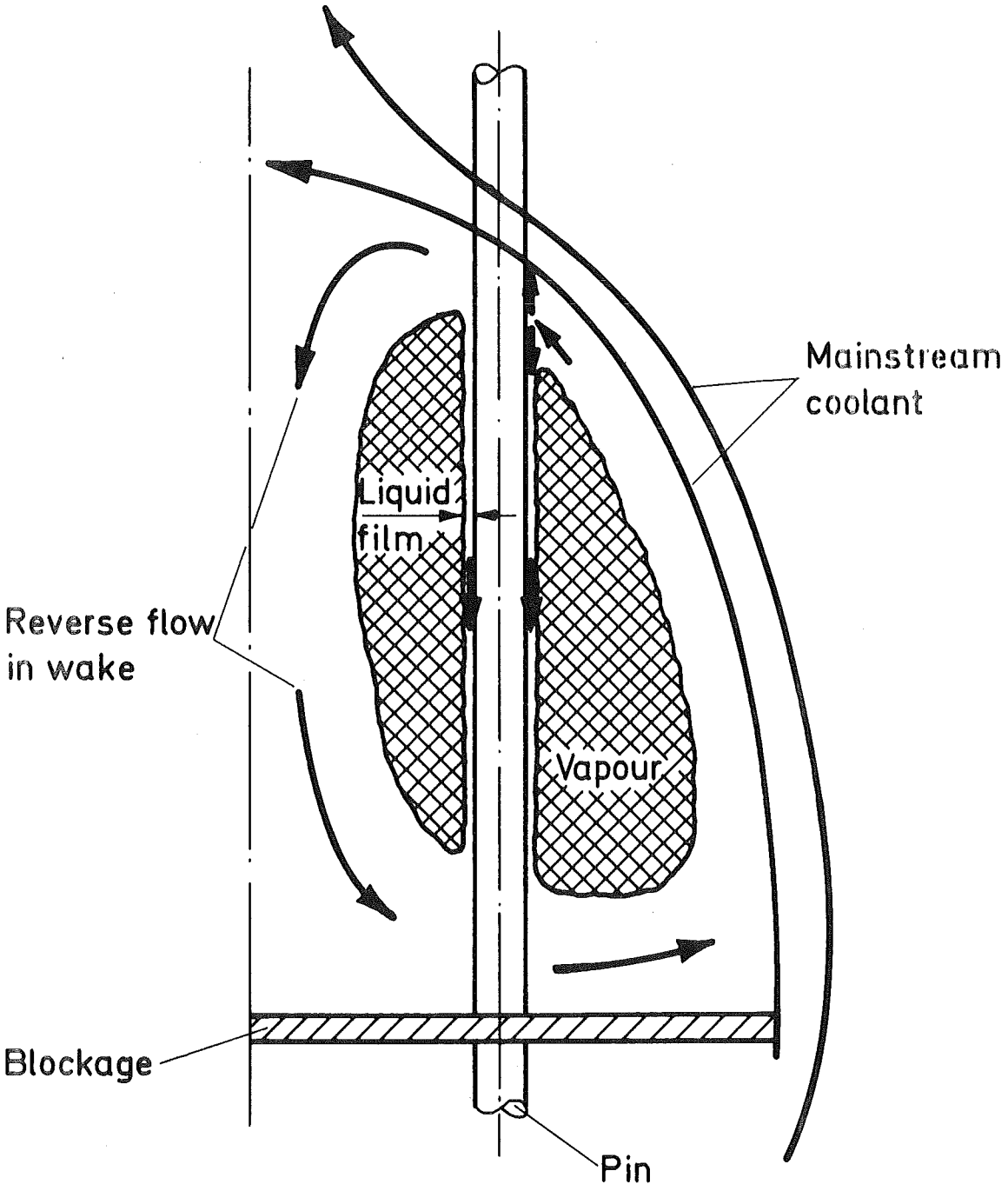

Fig.6 Diagram illustrating the draining film liquid source

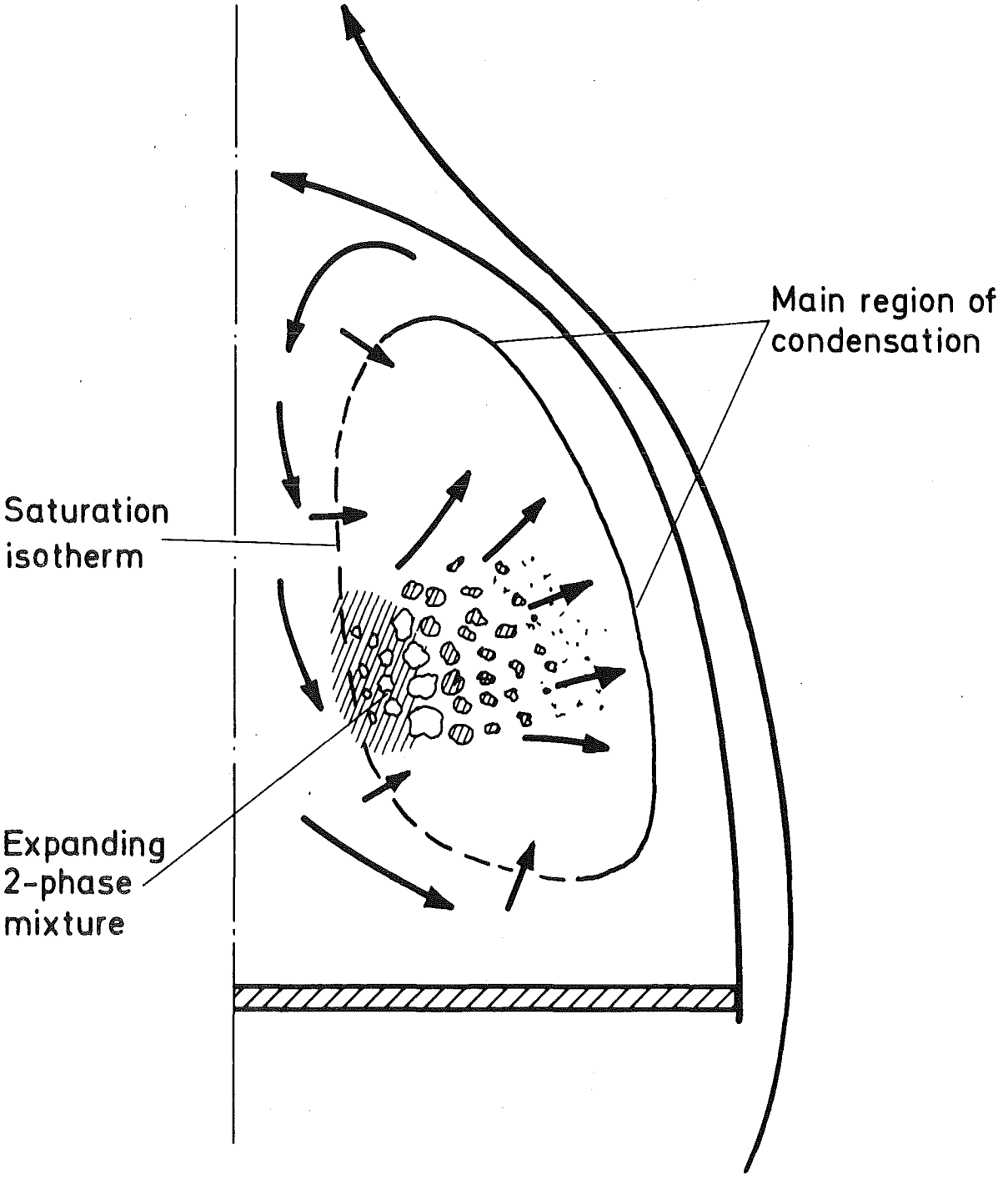

Fig.7 Illustration of the 2-phase mixture model

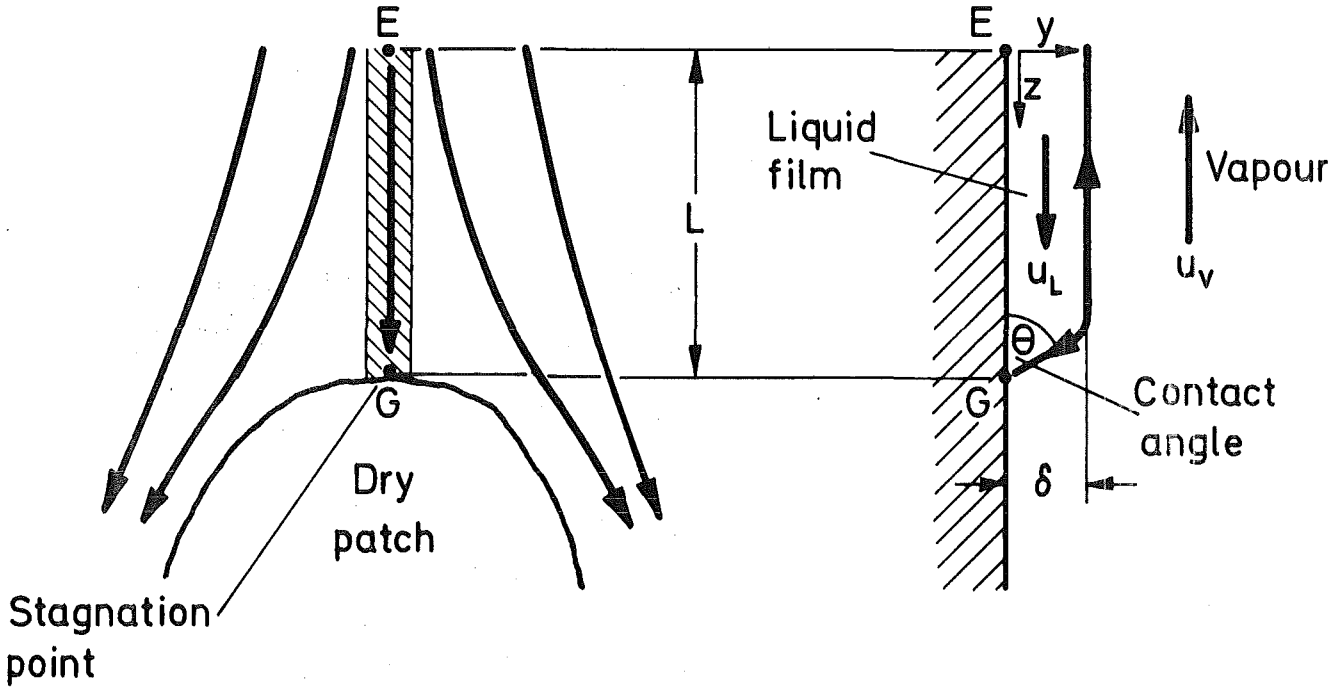

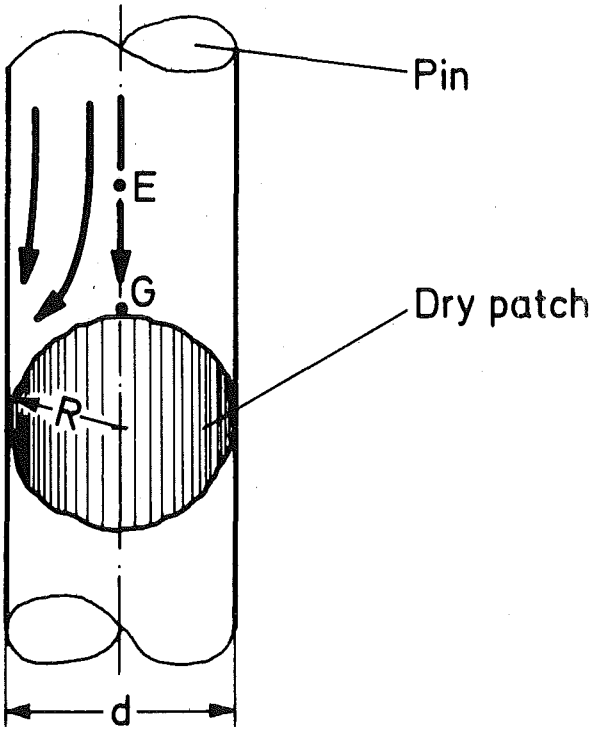

KfK

Fig.8 Explanatory diagram for dry patch stability analysis

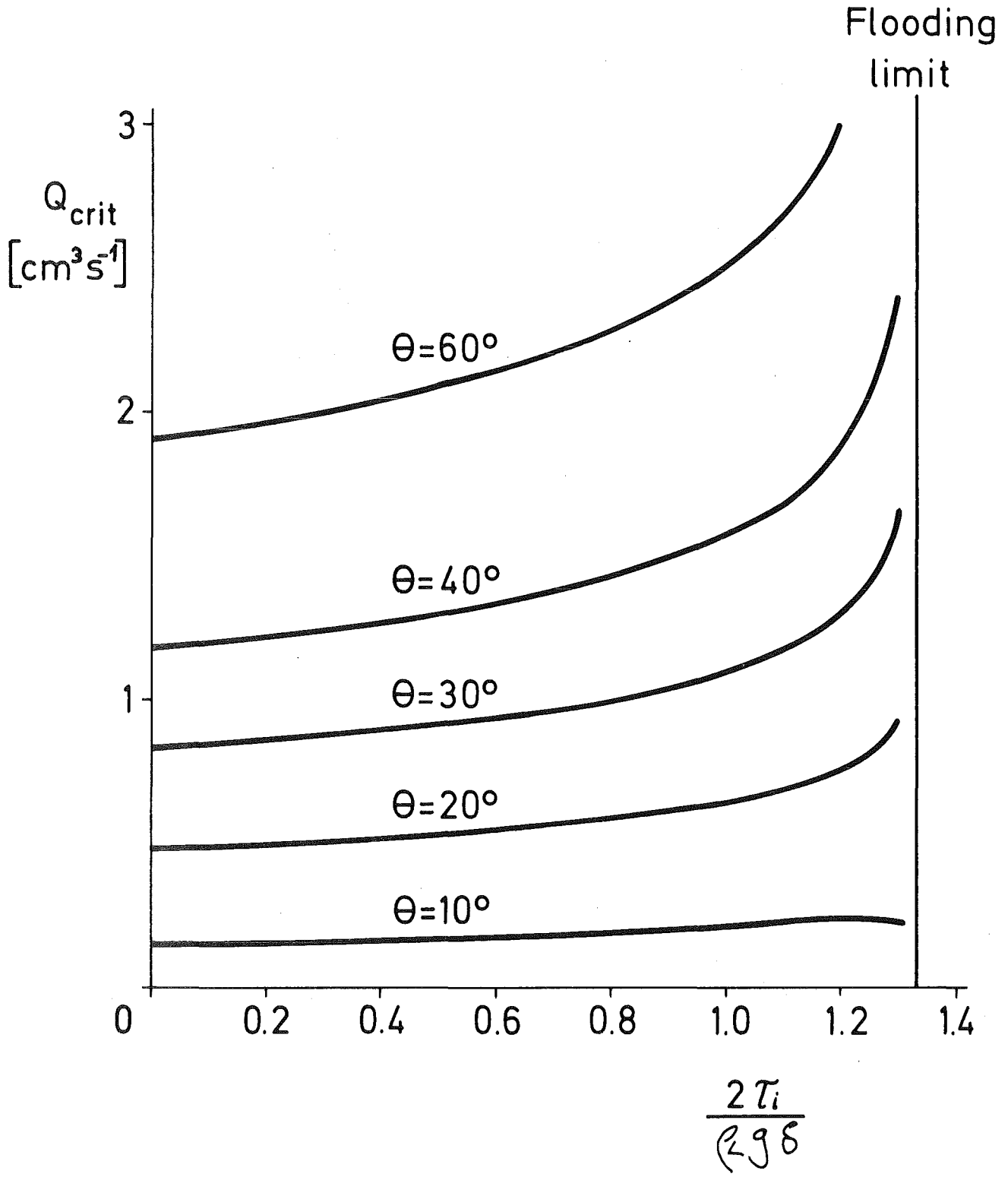

Fig.9 Hydrodynamic limit for dry patch rewetting with vapour counterflow

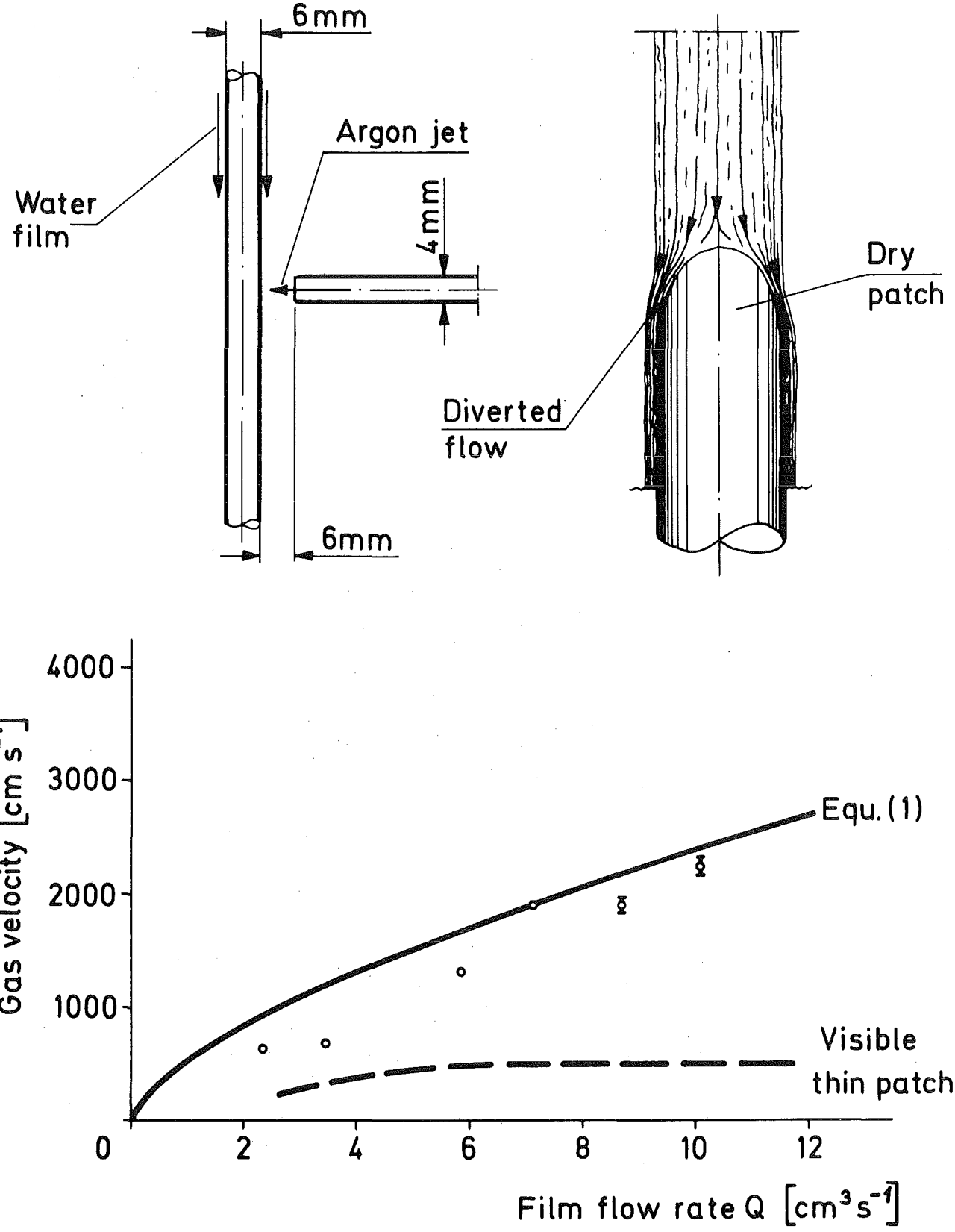

Fig.10 Breakdown of a draining water film by a gas jet

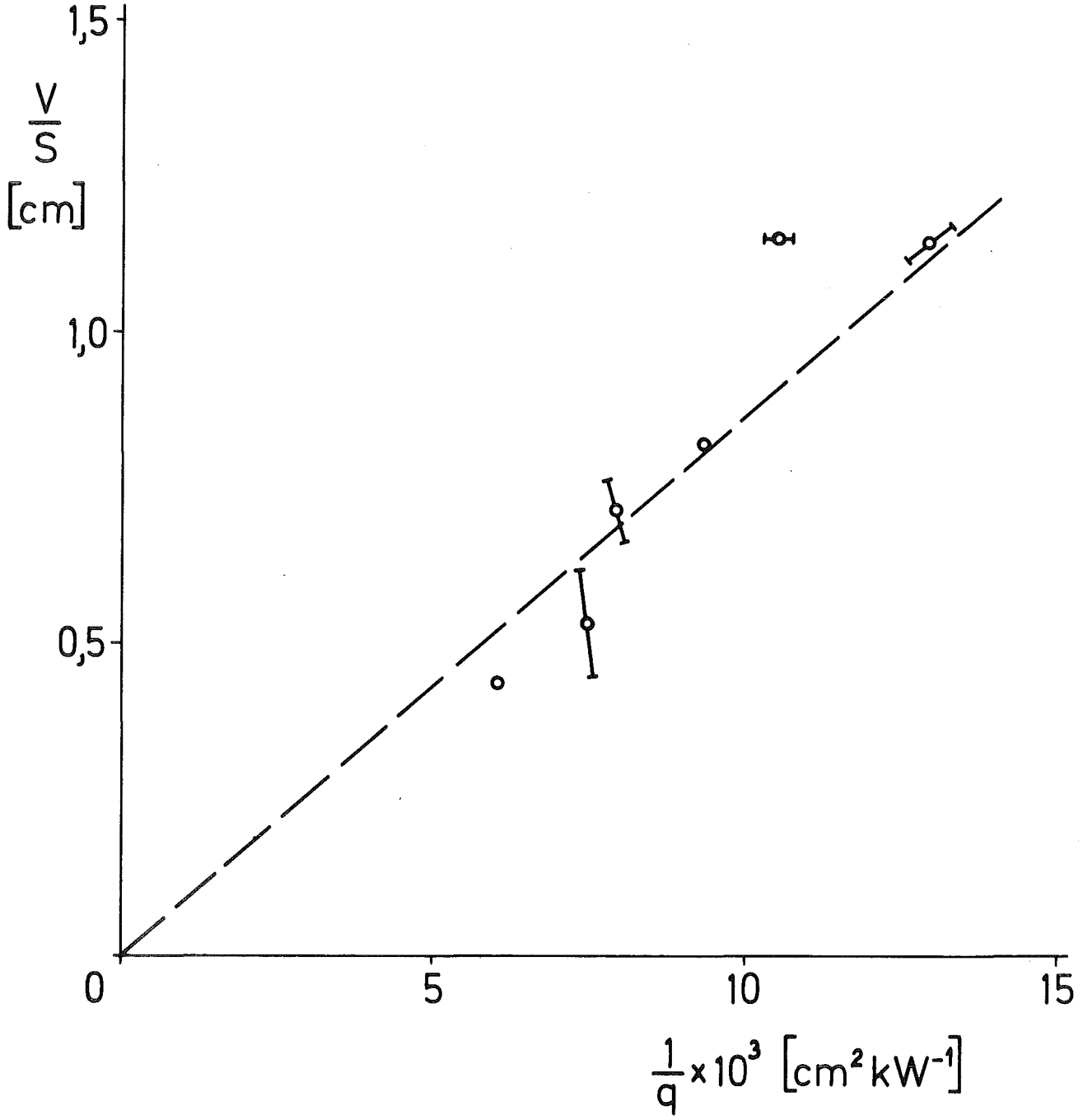

Fig.11 Volume/surface area ratio for vapour regions at dryout